

## Phase 2a Clinical Trial of Mitochondrial Protection (Elamipretide) During Stent Revascularization in Patients With Atherosclerotic Renal Artery Stenosis

Ahmed Saad, MD; Sandra M.S. Herrmann, MD; Alfonso Eirin, MD; Christopher M. Ferguson, MSc; James F. Glockner, MD, PhD; Haraldur Bjarnason, MD; Michael A. McKusick, MD; Sanjay Misra, MD; Lilach O. Lerman, MD, PhD; Stephen C. Textor, MD

**Background**—Atherosclerotic renal artery stenosis reduces renal blood flow (RBF) and amplifies stenotic kidney hypoxia. Revascularization with percutaneous transluminal renal angioplasty (PTRA) and stenting often fails to recover renal function, possibly because of ischemia/reperfusion injury developing after PTRA. Elamipretide is a mitochondrial-targeted peptide that binds to cardiolipin and stabilizes mitochondrial function. We tested the hypothesis that elamipretide plus PTRA would improve renal function, oxygenation, and RBF in patients with atherosclerotic renal artery stenosis undergoing PTRA.

**Methods and Results**—Inpatient studies were performed in patients with severe atherosclerotic renal artery stenosis scheduled for PTRA. Patients were treated before and during PTRA with elamipretide (0.05 mg/kg per hour intravenous infusion, n=6) or placebo (n=8). Stenotic kidney cortical/medullary perfusion and RBF were measured using contrast-enhanced multidetector CT, and renal oxygenation by 3-T blood oxygen level–dependent magnetic resonance imaging before and 3 months after PTRA. Age and basal glomerular filtration rate did not differ between groups. Blood oxygen level–dependent imaging demonstrated increased fractional hypoxia 24 hours after angiography and stenting in placebo (+47%) versus elamipretide (–6%). These were reverted to baseline 3 months later. Stenotic kidney RBF rose ( $202\pm 29$ – $262\pm 115$  mL/min;  $P=0.04$ ) 3 months after PTRA in the elamipretide-treated group only. Over 3 months, systolic blood pressure decreased, and estimated glomerular filtration rate increased ( $P=0.003$ ) more in the elamipretide group than in the placebo group ( $P=0.11$ ).

**Conclusions**—Adjunctive elamipretide during PTRA was associated with attenuated postprocedural hypoxia, increased RBF, and improved kidney function in this pilot trial. These data support a role for targeted mitochondrial protection to minimize procedure-associated ischemic injury and to improve outcomes of revascularization for human atherosclerotic renal artery stenosis.

**Clinical Trial Registration**—URL: <https://www.clinicaltrials.gov>. Unique identifier: NCT01755858.

(*Circ Cardiovasc Interv.* 2017;10:e005487. DOI: 10.1161/CIRCINTERVENTIONS.117.005487.)

**Key Words:** angioplasty ■ hypoxia ■ kidney ■ magnetic resonance imaging ■ renal artery stenosis ■ renovascular hypertension ■ reperfusion injury

Atherosclerotic renal artery stenosis (ARAS) reduces renal blood flow (RBF) and ultimately accentuates tissue hypoxia.<sup>1</sup> Although the kidneys can adapt to moderate reductions in blood flow without major loss of oxygenation,<sup>2</sup> severe reductions in RBF eventually lead to vascular rarefaction, inflammatory injury, and tissue fibrosis, which has been designated ischemic nephropathy.<sup>3</sup> Severe degrees of vascular occlusion are associated with overt cortical hypoxia,<sup>1,4</sup> oxidative stress, and loss of renal function.<sup>5–7</sup> Many of these changes fail to reverse after restoring vessel patency alone.<sup>7,8</sup>

### See Editorial by Kloner

The clinical benefits of revascularization procedures to restore blood flow in ARAS remain ambiguous. Although

some patients treated with stent revascularization achieve lower blood pressures and reduced medication requirements, kidney function infrequently improves and sometimes declines.<sup>9–11</sup> These observations raise concerns that abrupt reperfusion may induce a form of ischemia/reperfusion injury (IRI) in the kidney.

Experimental studies in swine ARAS suggest that renal revascularization triggers the release of inflammatory cytokines such as monocyte chemoattractant protein (MCP)-1<sup>12</sup> from the stenotic kidney (SK). MCP-1 is a primary mediator of inflammation, fibrosis, and microvascular rarefaction induced by hypertension.<sup>13</sup> Abrupt reperfusion can amplify tissue injury by upregulating inflammation and oxidative stress<sup>14</sup> characterized by rapid swelling and fragmentation

Received May 12, 2017; accepted July 24, 2017.

From the Division of Nephrology and Hypertension (A.S., S.M.S.H., A.E., C.M.F., L.O.L., S.C.T.) and Department of Radiology (J.F.G., H.B., M.A.M., S.M.), Mayo Clinic, Rochester, MN.

The Data Supplement is available at <http://circinterventions.ahajournals.org/lookup/suppl/doi:10.1161/CIRCINTERVENTIONS.117.005487/-/DC1>.

Correspondence to Stephen C. Textor, MD, Mayo Clinic, 200 First St, SW, Rochester, MN 55905. E-mail [stextor@mayo.edu](mailto:stextor@mayo.edu)

© 2017 American Heart Association, Inc.

*Circ Cardiovasc Interv* is available at <http://circinterventions.ahajournals.org>

DOI: 10.1161/CIRCINTERVENTIONS.117.005487

### WHAT IS KNOWN

- Reduced kidney function from ARAS often fails to recover after revascularization. Elamipretide is a mitochondria-targeted peptide shown to protect against experimental ischemic renal injury and improves renal outcomes after revascularization in experimental ARAS.

### WHAT THE STUDY ADDS

- Elamipretide during PTRAs attenuated renal hypoxia developing 24 hours after contrast imaging and renal artery stent revascularization. Cortical blood flow and estimated glomerular filtration rate increased in the elamipretide group when measured 3 months later.
- Adjunctive elamipretide during PTRAs was associated with increased peripheral venous levels of G1 cell cycle arrest markers IGFBP-7\*TIMP-2 at 24 hours after stenting.
- The rise of IGFBP-7 and TIMP-2 at 24 hours in the elamipretide group may reflect a protective role in the face of contrast and procedural hazards.

of mitochondria in the renal proximal tubule,<sup>15</sup> sustained energetic deficits,<sup>16</sup> and activation of cell death pathways.<sup>17</sup> Increased mitochondrial reactive oxygen species production is thought to be a major mechanism in the pathogenesis of IRI.<sup>18</sup> Reactive oxygen species cause peroxidation and loss of cardiolipin,<sup>19</sup> a phospholipid found in the inner mitochondrial membrane, leading to mitochondrial dysfunction.<sup>20</sup> Kidney ischemia is recognized to induce disruptions in mitochondrial function and ATP generation that can be partially abrogated by agents that stabilize mitochondrial cardiolipin.<sup>21,22</sup> Experimental studies have shown that cardiolipin protection before and during angioplasty (percutaneous transluminal renal angioplasty [PTRAs]) attenuates IRI-induced apoptosis and oxidative stress in animal models.<sup>12</sup>

Elamipretide (also known as MTP-131 or Bendavia) is a small peptide that targets the mitochondrial matrix independent of membrane potential, preventing peroxidation of cardiolipin.<sup>14,23,24</sup> Elamipretide has demonstrated potential for attenuating IRI in experimental models of acute kidney injury and improving kidney outcomes and restoring renal function after PTRAs in experimental ARAS.<sup>12</sup> However, its capability to modify outcomes after restoration RBF in humans with chronic renal ischemia is unknown. In this pilot study, we tested the hypothesis that elamipretide infusion immediately before and during renal revascularization would improve renal function, oxygenation, and RBF in ARAS patients undergoing PTRAs with stenting.

## Methods

### Patient Selection

In this phase 2a, randomized, double-blinded, placebo-controlled pilot study, we enrolled 14 patients with severe ARAS (estimated by renal artery Doppler ultrasound velocity acceleration [average peak systolic velocity >375 cm/s]) between December 2012 and September

2015. Patients were scheduled for renal revascularization for clinical indications, including resistant hypertension (systolic hypertension >150 mmHg and the use of at least 2 BP drugs) and declining renal function. Exclusion criteria were the following: serum creatinine >2.5 mg/dL, renal disease requiring dialysis, significant medical conditions (cancer, angina, or stroke) within the 6 months before administration of the drug and serum sodium <135 mmol/L on the day of the PTRAs. Patients were admitted to the Clinical Research Unit at St. Mary's Hospital, Rochester, MN, for a 3-day inpatient protocol on 2 occasions (before and 3 months after renal artery revascularization), as previously described.<sup>25</sup> All received agents blocking the renin-angiotensin system during these studies (angiotensin converting enzyme inhibitors or angiotensin receptor blockers). Since many patients had bilateral stenosis, 21 SKs were stented and available for analysis. Three patients had unilateral atrophic kidneys, leaving 4 nonstenotic (contralateral kidneys) available for analysis. Dietary intake was regulated at 150 mEq of sodium with an isocaloric diet prepared on site. Informed, written consent was obtained as approved by the institutional review board of the Mayo Clinic. During PTRAs, patients were assigned randomly to either elamipretide (0.05 mg/kg per hour, n=6) or identically prepared placebo (n=8) infusion, which started 30 minutes before PTRAs. All study personnel and patients were blinded to treatment.

### Renal Function and Blood Pressure Measurements

The morning of first study day included measurement of glomerular filtration rate (GFR) by iothalamate clearance (iothalamate meglumine, Conray, Mallinckrodt) after oral hydration (20 mL/kg) over three 30-minute timed collection periods.<sup>26,27</sup> Blood pressure was measured by automated oscillometric recordings, including 3 values taken 3× daily (an automated oscillometric unit, Omron blood pressure, measured blood pressure at 5, 7, and 9 minutes after a 5-minute rest).

### Renal Oxygenation Determined by Blood Oxygen Level–Dependent Magnetic Resonance Imaging

On the afternoon of the first and third days, blood oxygen level–dependent (BOLD) magnetic resonance imaging examinations were performed on a (GE Twin Speed Signa EXCITE) 3.0-T system (GE Medical Systems, Waukesha, WI) using a 12-channel torso-phased array coil.<sup>25</sup> BOLD imaging consisted of a 2-dimensional fast spoiled gradient echo sequence with multiple echo times. Parametric images of R2\* were generated by fitting signal intensity versus echo time data to an exponential function on a voxel-by-voxel basis and solving for R2\*.<sup>28</sup> After the first BOLD acquisition, furosemide (20 mg) was administered intravenously and flushed with 20 mL of saline. BOLD measurements for each kidney were repeated 15 minutes later. Analysis of BOLD data was performed by drawing parenchymal regions of interest on 2 to 4 slices through the midpole hilar region of each kidney on representative T2\*-weighted images and then transferring the region of interest to the corresponding R2\* parametric image as previously described.<sup>1</sup> To determine the portion of measured kidney area for which tissue hypoxia was present, we evaluated fractional tissue hypoxia by measuring the percentage of voxels from the whole-kidney region of interest with R2\* values >20 s<sup>-1</sup> (on coronal images) which mainly represents the medulla, taking the average of all available slices.<sup>1</sup> BOLD imaging was repeated 24 hours after renal artery stent placement and during the return protocol admission 3 months later.

### Cortical and Medullary Tissue Perfusion and Blood Flow Measured by Multidetector Computed Tomography

On the second study day, the common femoral vein was cannulated with a 6F sheath and blood samples drawn from the right and left renal veins with a 5F pigtail Cobra catheter (Cook, Inc, Bloomington, IN). The catheter was then advanced into the right atrium for central venous injection of contrast for flow studies using multidetector computed tomography (MDCT). For assessment of perfusion, MDCT imaging was performed using a dual-source 64-slice helical MDCT scanner (SOMATOM Definition, Siemens Medical Solutions) after a bolus injection of iopamidol 370 (0.5 mL/kg up to a maximum of 40

mL). Fifteen minutes after completion of the perfusion study, a kidney volume study (5-mm-thick slices) was performed in the helical mode to determine both cortical and medullary regional volumes. To calculate regional perfusions and volumes, images were reconstructed and displayed with the Analyze software package (Biomedical Imaging Resource, Mayo Clinic, MN). Regions of interest were selected from cross-sectional images from the aorta, renal cortex, and medulla. Average tissue attenuation in each region was plotted over time and fitted by curve-fitting algorithms to obtain measures of renal perfusion and function as described previously.<sup>29,30</sup>

### Elamipretide Infusion and Safety Monitoring

After completing MDCT imaging, patients were returned to the angiography suite where elamipretide or placebo infusion started for 30 minutes. All procedures were performed with the use of the same technique. The right common femoral artery was accessed with 18 gauge, 7-cm angiographic needle (Cook, Bloomington, IN). A 6F or 7F vascular sheath (Terumo, Somerset, NJ) was placed in the artery over a Bentsen guide wire (Cook). A 6F or 7F internal mammary guide catheter (Boston Scientific, Natick, MA) was used to engage the origin of the renal artery. Angiography was performed with 4 to 8 mL of Visipaque 320 (GE Healthcare, Princeton, NJ) to determine the extent of stenosis. Patients were typically given a bolus of heparin intravenously (50 U/kg of body weight) before the placement of the stent. The elamipretide or placebo infusion continued for 3 hours. After the stent deployment, a completion angiogram was performed to exclude segmental or intrarenal occlusion. The total contrast volume for both MDCT and angiography was less than  $\approx 100$ –120 mL.

Patients were followed for the next 24 hours after PTRAs with serial measurements of vital signs, serum sodium, MCP-1 (monocyte chemoattractant protein-1), IL-10 (interleukin-10), KIM-1 (kidney injury molecule), TNF- $\alpha$  (tumor necrosis factor- $\alpha$ ), IGFBP-7 (insulin-like growth factor-binding protein-7) or TIMP-2 (tissue inhibitor of metalloproteinases-2), and NGAL (neutrophil gelatinase-associated lipocalin). Collected samples were centrifuged, and the supernatant stored at  $-80^{\circ}\text{C}$  until measurement. NGAL and KIM-1 (ng/mL) were tested by ELISA according to the manufacturer's protocol (BioPorto Diagnostics, Cat no. KIT 036 and R&D systems, Cat no. DKM100, respectively). The samples for IGFBP-7 were diluted 1:2 and tested by ELISA (R&D systems, Cat no. KIT DY1334-05). The samples for TIMP-2 were diluted 1:500 and tested by ELISA (Sigma-Aldrich, lot no. RAB0472). Levels of TNF- $\alpha$  and MCP-1 were measured by Luminox (Millipore, Cat no. MPXHCYTO-60K). Signals were read by the Bio-plex 200 systems (BIO-RAD).

### Statistical Analysis

Results were expressed using mean values and SD or median values (interquartile range), as appropriate. Qualitative variables were expressed as number (percentage). Because several patients had bilateral disease and stenting, our analysis accounted for the clustering within subjects by running repeated measures linear regression with a random intercept for each patient.  $\chi^2$  test or Fisher exact test was used for categorical variables as appropriate. Comparisons between individual kidneys before and after treatment and changes over time in the 2 treatment groups were performed using repeated measures models. Percent (%) change in SK-fractional hypoxia was calculated as follows:  $[(3\text{-month SK-}\%R2^{*}>20\text{-baseline SK-}\%R2^{*}>20)/\text{baseline SK-}\%R2^{*}>20] \times 100\%$ . Statistical significance was accepted for  $P \leq 0.05$ . Statistical analysis was performed using JMP software package version 8.0 (SAS Institute Inc, Cary, NC).

## Results

### Demographic Comparison Between ARAS Patients

Complete data were available for 14 ARAS patients included in the elamipretide ( $n=6$ ) and placebo ( $n=8$ ) groups. The demographic and clinical features of the patients studied are summarized in Table 1. Age, sex, serum creatinine, GFR, and blood pressure were not different between groups.

**Table 1. Clinical, Laboratory, and Demographic Data of EH ARAS Patients**

	Elamipretide (n=6)	Placebo (n=8)	P Value
Gender (%men)*	3 (50%)	4 (50%)	0.99
Age, y	66.7 $\pm$ 6.8	72.5 $\pm$ 8.1	0.17
Creatinine, mg/dL	1.58 $\pm$ 0.36	1.83 $\pm$ 0.52	0.32
Iothalamate clearance, mL/min	46.8 $\pm$ 24.5	43.6 $\pm$ 12.3	0.99
Statins (yes/no) (%)*	5/1 (83%)	5/3 (63%)	0.58
No. of anti-HTN drugs†	3.5 (2, 5)	4 (2, 6)	0.44
SBP, mm Hg	154.2 $\pm$ 16.3	155.2 $\pm$ 19.5	0.92
DBP, mm Hg	79.2 $\pm$ 9.1	72.5 $\pm$ 15.4	0.33
Weight, kg	90.7 $\pm$ 35.3	83.8 $\pm$ 14.6	0.66
BMI, kg/m <sup>2</sup>	33 $\pm$ 12.5	29.4 $\pm$ 3.9	0.51
Hematocrit %	37.3 $\pm$ 2.6	36.2 $\pm$ 2.5	0.42

Mean $\pm$ SD. ARAS indicates atherosclerotic renal artery stenosis; BMI, body mass index; DBP, diastolic blood pressure; HTN, hypertensive; and SBP, systolic blood pressure.

\*Fisher exact test.

†Median (range) reported because of skewed data; P value obtained from Wilcoxon rank-sum test.

### Safety Monitoring: Sequential Measurements After Elamipretide Infusion

All patients tolerated the single elamipretide infusion without identified adverse clinical effects including fever, headache, vomiting, hematuria, or allergic reactions. Over the 24 hours after infusion of elamipretide, there were no changes in serum creatinine or urine cytology.

### Adjunctive Elamipretide During PTRAs Was Associated With Attenuated Postprocedural Hypoxia

Tissue oxygenation levels defined both by cortical  $R2^{*}$  values and fractional hypoxia did not differ between groups at baseline. Twenty-four hours after PTRAs and contrast-enhanced CT, overt cortical and fractional tissue hypoxia developed in both groups in 9 patients (64%). The degree of poststenting hypoxia was attenuated in the elamipretide group (fractional hypoxia  $\%R2^{*}>20\text{ s}^{-1}$  from  $45 \pm 17$  to  $52.4$ ;  $P=0.42$ ), whereas a rise was observed in the placebo group ( $50.9 \pm 18.6$ – $67.7 \pm 27.1$ ;  $P=0.03$ ; Table 2). When expressed as percent (%) change from baseline, the SK-fractional hypoxia in the elamipretide group was unchanged at 24 hours ( $-5.9\%$ ) but increased in the placebo group (47%). These levels of tissue hypoxia reversed to baseline levels at 3 months in both groups (Figure I in the [Data Supplement](#)). Representative BOLD images ( $R2^{*}$  parametric maps) illustrating the change in hypoxia in an SK from each treatment group before and 24 hours after PTRAs are illustrated in Figure 1.

### Adjunctive Elamipretide During PTRAs Was Associated With Increased RBF and Cortical Perfusion After 3 Months

Results from quantitative MDCT measurements of hemodynamics for individual SKs at baseline and after 3 months are summarized in Table 3. The total SK volume did not change in either placebo or elamipretide groups, whereas

**Table 2. Blood Oxygen Level–Dependent Magnetic Resonance Imaging for Stenotic Kidney Before and 24 Hours After Revascularization Using Fractional Tissue Hypoxia and Cortical Regions of Interest Measurements**

Single Kidney		Elamipretide (n=10)		Placebo (n=11)	
		Baseline	After 24 h	Baseline	After 24 h
Cortex R2*, s <sup>-1</sup> )	Pre-furosemide	19.4±2.7	20.1±4.4	19.9±3.4	24.4±6.2*
	Post-furosemide	18.3±2.6†	19.8±5.1	19.5±3.9	23.7±6.8*†
Percent change in cortex R2* at 24 h	Pre-furosemide	–3 (–10, 24.8)		13 (–0.5, 31.9)	
	Post-furosemide	–0.8 (–14.9, 37)		11.1 (–0.02, 39)	
Fractional hypoxia (% R2* >20 s <sup>-1</sup> )	Pre-furosemide	45±17	52.4±28.9	50.9±18.6	67.7±27.1*
	Post-furosemide	31.9±12.8†	44.2±26.4†	41±22.8†	58.3±36.6
Percent change in fractional hypoxia %>20 s <sup>-1</sup> at 24 h	Pre-furosemide	–5.9 (–34.5, 96.2)		47 (–2.2, 74.9)	
	Post-furosemide	13 (–31, 133.5)		44 (–48.4, 109.7)	

\**P*<0.05 vs baseline.†*P*<0.05 vs pre-furosemide (from repeated measures regression model).

total RBF and cortical blood flow increased only in the elamipretide group (Figure 2). Cortical perfusion in the SKs rose in the elamipretide group (from 1.99±0.8 to 2.9±1 mL/min per mL of tissue; *P*=0.04) but remained unchanged in the placebo group.

#### Adjunctive Elamipretide During PTRAs Was Associated With Increased GFR After 3 Months

Serum creatinine decreased 3 months after PTRAs (from 1.58±0.36 to 1.4±1.34 mg/dL; *P*=0.0005) in the elamipretide group and was unchanged in the placebo group (from 1.8±0.5 to 1.7±0.4 mg/dL; *P*=0.13). As a result, estimated GFR increased (from 40.7±13.4 to 46.5±15 mL/min per 1.73 m<sup>2</sup>; *P*=0.002) in the elamipretide group and (from 34.4±9.5 to 37±10.5 mL/min per 1.73 m<sup>2</sup>; *P*=0.24) in the placebo group (Figure 3). Systolic blood pressure decreased (from 154±16 to 133±16.8 mm Hg; *P*=0.03) in the elamipretide group but less (from 154±18.5 to 143.7±26; *P*=0.06) in the placebo group.

#### Adjunctive Elamipretide During PTRAs Was Associated With Transiently Increased Cell Cycle Arrest Markers IGFBP-7×TIMP-2

Twenty-four hours after PTRAs (reperfusion), peripheral vein levels of IGFBP-7×TIMP-2 increased only in the elamipretide group (Figure 4) but decreased again at 3 months, whereas NGAL levels decreased at 24 hours in both groups then rose up again to baseline levels at 3 months in both groups (Table I in the [Data Supplement](#)). There were no changes in the IL-10, MCP-1, and TNF-α levels.

#### Discussion

The results of this phase 2a, randomized, double-blinded, placebo-controlled pilot study indicate that adjunctive intravenous elamipretide (a mitochondria-targeted peptide) during PTRAs attenuated renal hypoxia developing 24 hours after contrast imaging and renal artery stent revascularization. Adjunctive elamipretide was associated with increased cortical perfusion and RBF in the stented kidney after 3 months in patients

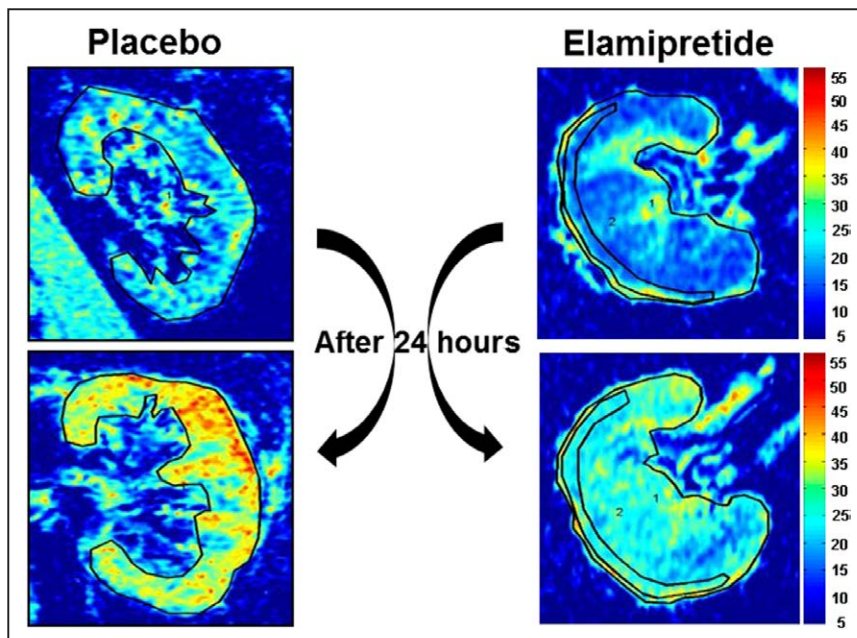


**Figure 1.** Examples of R2\* parametric maps (coronal plane) for subjects with atherosclerotic renal artery stenosis (ARAS) at baseline and 24 hours after contrast imaging and percutaneous transluminal renal angioplasty (PTRAs), obtained using the same color scale for R2\*, demonstrating the transient widespread tissue hypoxia developed 24 hours after contrast imaging and renal stenting. Adjunctive elamipretide during PTRAs attenuated postprocedural hypoxia.

**Table 3. Multidetector CT Measurements of Individual Kidney Volume, Tissue Perfusion, Blood Flow, and Iothalamate Filtration of SK**

Single Kidney, SK	Elamipretide (n=10)		Placebo (n=11)	
	Baseline	3 mo	Baseline	3 mo
Total kidney volume (CT), mL	124.7±50	127.8±54	115.6±46.7	112.5±46.9
Cortical volume, mL	71.6±30.3	76±32	68.8±30.6	71.3±30.6
Medullary volume, mL	53.1±22	51.8±23	46.8±17.4	41.2±17.5
Cortical perfusion, mL/min per mL of tissue	1.99±0.8	2.9±1.04*	2.6±0.9	2.4±0.39
Medullary perfusion, mL/min per mL of tissue	0.75±0.37	0.95±0.4	0.92±0.4	0.89±0.2
Total renal blood flow, mL/min	202±129	261.7±115*	234±133	234±99
Cortical flow, mL/min	157±99	212±93.1*	189±111	194.9±87
Medullary flow, mL/min	44.6±36.9	49.7±35	45.1±27.7	39±15

SK indicates stenotic kidney.

\* $P < 0.05$  vs baseline (paired *t* test and Wilcoxon signed-rank test).

with ARAS when compared with placebo. These changes in the elamipretide-treated patients were associated with reductions in systolic blood pressure and greater increase in total GFR. The results of this study support further development of mitochondrial-targeted therapies to limit procedure-associated hypoxia and potentially to improve kidney functional outcomes of revascularization in patients with ARAS.

Renal stenting alone often fails to restore kidney function in ARAS, as reported in multiple recent clinical trials.<sup>10,11</sup> Our experimental studies in swine models of RAS demonstrate loss of microvascular structures<sup>31</sup> that is magnified in the atherosclerotic environment<sup>5,32,33</sup> and correlates with loss of GFR.<sup>8,34</sup> Loss of cortical structural integrity appears in part related to oxidative stress, ATP depletion, and mitochondrial damage,<sup>22,31</sup> which do not reverse after revascularization alone.<sup>7,8</sup> Although restoring blood flow may be needed to prevent further ischemic damage, abrupt restoration of blood flow also may injure cells that are hovering between life and death.<sup>14</sup> Abrupt reperfusion accentuates tissue injury by upregulating inflammatory signals like MCP-1, oxidative stress, or other injurious pathways<sup>12</sup> that define IRI. Reperfusion also increases production of mitochondrial  $\text{Ca}^{2+}$  and reactive oxygen species, opening the mitochondrial permeability transition pore in the inner mitochondrial membrane, leading to release

of cytochrome *c* into the cytosol and cardiolipin peroxidation.<sup>35,36</sup> Cardiolipin is a bisphosphatidyl glycerol lipid exclusively distributed in the inner mitochondrial membrane that regulates multiple mitochondrial activities, including electron transport chain assembly and function, ATP biosynthesis, and apoptosis.<sup>37</sup> The changes instigated during IRI in turn may induce mitochondrial dysfunction, apoptosis, inflammation, fibrosis, and renal dysfunction.

Elamipretide is a tetrapeptide that selectively concentrates in the inner mitochondrial membrane, where it binds to and stabilizes cardiolipin and prevents its peroxidation.<sup>22</sup> This facilitates electron transport and inhibits mitochondrial permeability transition pore opening, attenuating apoptosis and experimental myocardial IRI.<sup>22,38</sup> Infusion of elamipretide during revascularization of the stenotic renal artery in swine ARAS reduces oxidative stress, tubular damage, and inflammation, thereby improving revascularization outcomes.<sup>12</sup> Previous studies in human ARAS have identified the development of widespread transient renal hypoxia lasting at least 24 hours after contrast imaging and PTRAs.<sup>39</sup> Our results extend the experimental studies of mitochondrial protection with elamipretide to human subjects. These data demonstrate that elamipretide reduced postprocedural hypoxia, as measured by BOLD magnetic resonance imaging 24 hours after PTRAs.

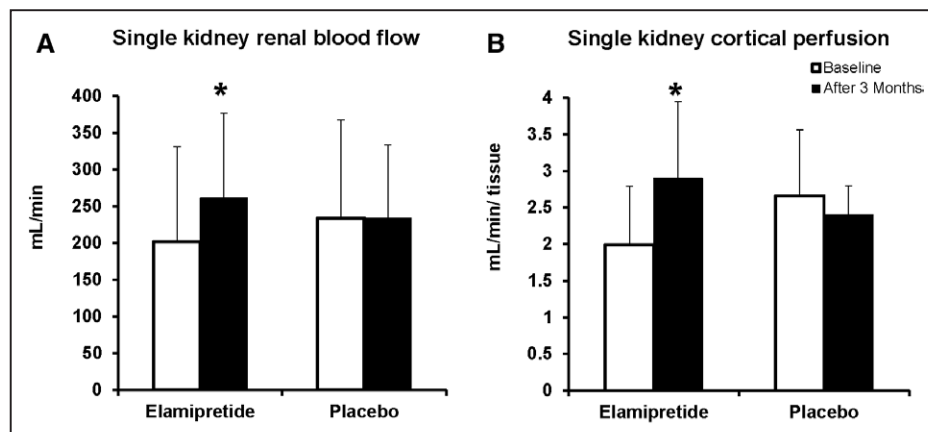


**Figure 2.** Adjunctive elamipretide during percutaneous transluminal renal angioplasty (PTRAs) was associated with increased renal blood flow (RBF; mL/min; **A**) at 3 months ( $P < 0.05$ ) and cortical perfusion (mL/min/cc of tissue; **B**).

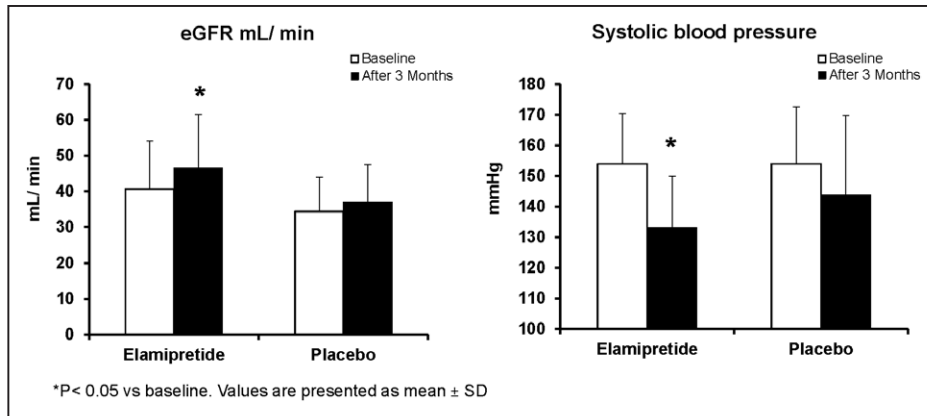


**Figure 3.** Adjunctive elamipretide during percutaneous transluminal renal angioplasty (PTRA) was associated with a greater rise in estimated GFR and decline in systolic blood pressure after 3 months when compared with placebo-treated subjects.

Remarkably, peripheral vein levels of IGFBP-7 and TIMP-2 rose after imaging and PTRA in the elamipretide group. IGFBP-7 and TIMP-2 have been proposed as markers in early diagnosis and prognostic prediction in acute kidney injury.<sup>40,41</sup> Both participate in G1 cell cycle arrest. When cell damage occurs from ischemia or sepsis, renal tubular cells enter a short period of G1 cell cycle arrest that prevents cells from dividing until the damage has been repaired.<sup>42</sup> We speculate that the rise of IGFBP-7 and TIMP-2 at 24 hours in the elamipretide group may reflect a protective role in the face of contrast and procedural hazards. The precise actions and role of NGAL in ARAS remain incompletely understood. While often presented as a marker of acute injury, NGAL itself is an anti-inflammatory cytokine that may limit tissue injury.<sup>43</sup> Administration of NGAL provides structural and functional protection in animal models and participates in regeneration and repair processes observed after injury.<sup>44</sup> We interpret our results demonstrating a rise of G1 cell cycle arrest markers and transient reductions in peripheral NGAL after imaging and PTRA in patients with chronic renal ischemia may have limited reperfusion injury. These changes in the elamipretide group were associated with reduced acute changes in tissue hypoxia and no evidence of tissue injury (as reflected by NGAL and creatinine).

Taken together, we interpret the enhanced kidney perfusion, blood flow, and recovery of GFR in the elamipretide group after renal artery stenting to support a role for mitochondrial protection in this condition. These data extend results in experimental

swine ARAS studies, in which mitochondrial biogenesis was upregulated in post-SKs of pigs treated with elamipretide, whereas oxidative stress, apoptosis, microvascular loss, and tissue injury were ameliorated 4 weeks after revascularization.<sup>12</sup>

Administration of elamipretide protects against reperfusion injury in several models of cardiac injury.<sup>45</sup> It also improves post-myocardial infarction cardiac function, prevents infarct expansion and adverse left ventricular remodeling, and reduced reactive oxygen species and cardiomyocytes apoptosis in the noninfarcted myocardial infarction border in rats.<sup>46</sup> Experimental studies of elamipretide infusion during renal revascularization improves myocardial mitochondrial biogenesis, cardiac function, and oxygenation and attenuates myocardial remodeling 4 weeks later.<sup>47</sup> Elamipretide also prevents cardiac remodeling and diastolic dysfunction in a mouse model of angiotensin-II-induced cardiomyopathy.<sup>38</sup> These studies suggest a potential for this compound to attenuating hypertensive myocardial injury. Despite efficacy in animal models, administration of elamipretide to patients with first time anterior ST-segment elevation myocardial infarction 10 minutes before percutaneous coronary intervention was not associated with a decrease in myocardial infarct size as assessed by AUC0-72 of creatinine kinase-MB enzyme.<sup>46</sup> The reasons for the lack of benefit after cardiac reperfusion are not clear. These differences underscore potential differences in injury associated with cardiac and renal reperfusion, as well as major species effects.

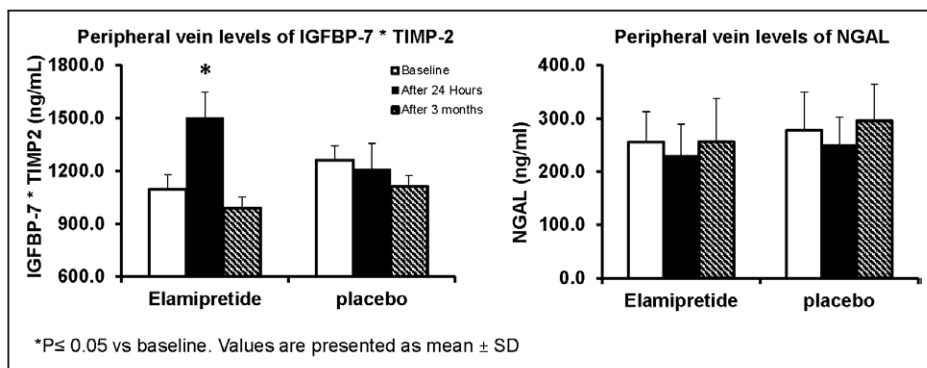


**Figure 4.** Adjunctive elamipretide during percutaneous transluminal renal angioplasty (PTRA) was associated with increased peripheral vein levels of IGFBP-7 (insulin-like growth factor-binding protein-7)\*TIMP-2 (tissue inhibitor of metalloproteinases-2) at 24 hours after stenting ( $P < 0.05$ ) that fell after 3 months. Neutrophil gelatinase-associated lipocalin (NGAL) levels fell transiently after 24 hours in both groups.

This study has limitations. It has relatively small number of patients. Enrolled patients were selected for revascularization based on clinical criteria. Revascularization and contrast injection were performed as part of a single procedure and either or both could contribute to the development of tissue hypoxia after 24 hours. Half the patients had bilateral stenosis with slightly less renal function. The BOLD magnetic resonance imaging parameter,  $R2^*$  used as a marker for tissue  $PO_2$ , can be affected slightly by variations in  $R2$  ( $=1/T2$ ) due to changes in water content,<sup>48</sup> although our patients were uniformly hydrated. Although the second BOLD magnetic resonance imaging was done 24 hours after contrast administration, we cannot exclude the possibility that some contrast retention within the kidney could affect the  $R2$ .<sup>49</sup> Studies of water loading in normal volunteers demonstrated a change in cortical  $R2$  of  $0.72\text{ s}^{-1}$ , whereas  $R2^*$  fell by  $1.36\text{ s}^{-1}$ . The observed cortical changes in  $R2^*$  in our patients were considerably greater (averaged  $4.5\text{ s}^{-1}$ ) making it likely that  $R2$  changes alone would be minor. Future studies might include  $R2$  mapping to allow for better interpretation of changes observed with  $R2^*$ .<sup>48</sup>

## Conclusions

Our results indicate that transient hypoxia developing after renal artery stenting was attenuated by elamipretide in patients with ARAS. Adjunctive elamipretide before and during PTRAs was associated with increased RBF and cortical perfusion, and estimated GFR by 3 months later, that were not apparent in control subjects. These pilot data support a role for targeted mitochondrial protection to improve outcomes of PTRAs for human ARAS.

## Sources of Funding

This project was partly supported by a grant from Stealth Peptides, Inc; R01 DK100081, DK10232, DK106427, and R01 DK 73608 from the National Institute for Digestive, Diabetic and Kidney Diseases; and Clinical and Translational Science Award (Grant UL1 RR024150) from National Institutes of Health/National Center for Research Resources (NCRR). The content is solely the responsibility of the authors and does not represent the official views of the National Institute for Digestive, Diabetic and Kidney Diseases or the National Institutes of Health.

## Disclosures

None.

## References

- Saad A, Crane J, Glockner JF, Herrmann SM, Friedman H, Ebrahimi B, Lerman LO, Textor SC. Human renovascular disease: estimating fractional tissue hypoxia to analyze blood oxygen level-dependent MR. *Radiology*. 2013;268:770–778. doi: 10.1148/radiol.13122234.
- Gloviczki ML, Glockner JF, Lerman LO, McKusick MA, Misra S, Grande JP, Textor SC. Preserved oxygenation despite reduced blood flow in poststenotic kidneys in human atherosclerotic renal artery stenosis. *Hypertension*. 2010;55:961–966. doi: 10.1161/HYPERTENSIONAHA.109.145227.
- Garovic VD, Textor SC. Renovascular hypertension and ischemic nephropathy. *Circulation*. 2005;112:1362–1374. doi: 10.1161/CIRCULATIONAHA.104.492348.
- Gloviczki ML, Lerman LO, Textor SC. Blood oxygen level-dependent (BOLD) MRI in renovascular hypertension. *Curr Hypertens Rep*. 2011;13:370–377. doi: 10.1007/s11906-011-0218-7.
- Chade AR, Rodriguez-Portel M, Grande JP, Krier JD, Lerman A, Romero JC, Napoli C, Lerman LO. Distinct renal injury in early atherosclerosis and renovascular disease. *Circulation*. 2002;106:1165–1171.
- Chade AR, Krier JD, Rodriguez-Portel M, Breen JF, McKusick MA, Lerman A, Lerman LO. Comparison of acute and chronic antioxidant interventions in experimental renovascular disease. *Am J Physiol Renal Physiol*. 2004;286:F1079–F1086. doi: 10.1152/ajprenal.00385.2003.
- Saad A, Herrmann SM, Crane J, Glockner JF, McKusick MA, Misra S, Eirin A, Ebrahimi B, Lerman LO, Textor SC. Stent revascularization restores cortical blood flow and reverses tissue hypoxia in atherosclerotic renal artery stenosis but fails to reverse inflammatory pathways or glomerular filtration rate. *Circ Cardiovasc Interv*. 2013;6:428–435. doi: 10.1161/CIRCINTERVENTIONS.113.000219.
- Eirin A, Ebrahimi B, Zhang X, Zhu XY, Tang H, Crane JA, Lerman A, Textor SC, Lerman LO. Changes in glomerular filtration rate after renal revascularization correlate with microvascular hemodynamics and inflammation in swine renal artery stenosis. *Circ Cardiovasc Interv*. 2012;5:720–728. doi: 10.1161/CIRCINTERVENTIONS.112.972596.
- Safian RD, Maddler RD. Refining the approach to renal artery revascularization. *JACC Cardiovasc Interv*. 2009;2:161–174. doi: 10.1016/j.jcin.2008.10.014.
- Wheatley K, Ives N, Gray R, Kalra PA, Moss JG, Baigent C, Carr S, Chalmers N, Eadington D, Hamilton G, Lipkin G, Nicholson A, Scoble J. Revascularization versus medical therapy for renal-artery stenosis. *N Engl J Med*. 2009;361:1953–1962.
- Cooper CJ, Murphy TP, Cutlip DE, Jamerson K, Henrich W, Reid DM, Cohen DJ, Matsumoto AH, Steffes M, Jaff MR, Prince MR, Lewis EF, Tuttle KR, Shapiro JI, Rundback JH, Massaro JM, D'Agostino RB, Sr, Dworkin LD; CORAL Investigators. Stenting and medical therapy for atherosclerotic renal-artery stenosis. *N Engl J Med*. 2014;370:13–22. doi: 10.1056/NEJMoa1310753.
- Eirin A, Li Z, Zhang X, Krier JD, Woollard JR, Zhu XY, Tang H, Herrmann SM, Lerman A, Textor SC, Lerman LO. A mitochondrial permeability transition pore inhibitor improves renal outcomes after revascularization in experimental atherosclerotic renal artery stenosis. *Hypertension*. 2012;60:1242–1249. doi: 10.1161/HYPERTENSIONAHA.112.199919.
- Lin J, Zhu X, Chade AR, Jordan KL, Lavi R, Daghini E, Gibson ME, Guglielmotti A, Lerman A, Lerman LO. Monocyte chemoattractant proteins mediate myocardial microvascular dysfunction in swine renovascular hypertension. *Arterioscler Thromb Vasc Biol*. 2009;29:1810–1816. doi: 10.1161/ATVBAHA.109.190546.
- Nilakantan V, Hilton G, Maenpaa C, Van Why SK, Pieper GM, Johnson CP, Shames BD. Favorable balance of anti-oxidant/pro-oxidant systems and ablated oxidative stress in brown Norway rats in renal ischemia-reperfusion injury. *Mol Cell Biochem*. 2007;304:1–11. doi: 10.1007/s11010-007-9480-z.
- Hall AM, Rhodes GJ, Sandoval RM, Corridon PR, Molitoris BA. In vivo multiphoton imaging of mitochondrial structure and function during acute kidney injury. *Kidney Int*. 2013;83:72–83. doi: 10.1038/ki.2012.328.
- Weinberg JM, Venkatachalam MA, Roeser NF, Nissim I. Mitochondrial dysfunction during hypoxia/reoxygenation and its correction by anaerobic metabolism of citric acid cycle intermediates. *Proc Natl Acad Sci USA*. 2000;97:2826–2831.
- Brooks C, Wei Q, Cho SG, Dong Z. Regulation of mitochondrial dynamics in acute kidney injury in cell culture and rodent models. *J Clin Invest*. 2009;119:1275–1285. doi: 10.1172/JCI37829.
- Plotnikov EY, Kazachenko AV, Vyssokikh MY, Vasileva AK, Tcvirkun DV, Isaev NK, Kirpatovsky VI, Zorov DB. The role of mitochondria in oxidative and nitrosative stress during ischemia/reperfusion in the rat kidney. *Kidney Int*. 2007;72:1493–1502. doi: 10.1038/sj.ki.5002568.
- Wiswedel I, Gardemann A, Storch A, Peter D, Schild L. Degradation of phospholipids by oxidative stress—exceptional significance of cardiolipin. *Free Radic Res*. 2010;44:135–145.
- Eirin A, Ebrahimi B, Zhang X, Zhu XY, Woollard JR, He Q, Textor SC, Lerman A, Lerman LO. Mitochondrial protection restores renal function in swine atherosclerotic renovascular disease. *Cardiovasc Res*. 2014;103:461–472. doi: 10.1093/cvr/cvu157.
- Szeto HH, Liu S, Soong Y, Wu D, Darrach SF, Cheng FY, Zhao Z, Ganger M, Tow CY, Seshan SV. Mitochondria-targeted peptide accelerates ATP recovery and reduces ischemic kidney injury. *J Am Soc Nephrol*. 2011;22:1041–1052. doi: 10.1681/ASN.2010080808.
- Birk AV, Liu S, Soong Y, Mills W, Singh P, Warren JD, Seshan SV, Pardee JD, Szeto HH. The mitochondrial-targeted compound SS-31 re-energizes ischemic mitochondria by interacting with cardiolipin. *J Am Soc Nephrol*. 2013;24:1250–1261. doi: 10.1681/ASN.2012121216.
- Sweetwyne MT, Pippin JW, Eng DG, Hudkins KL, Chiao YA, Campbell MD, Marcinek DJ, Alpers CE, Szeto HH, Rabinovitch PS, Shankland SJ. The mitochondrial-targeted peptide, SS-31, improves glomerular architecture in mice of advanced age. *Kidney Int*. 2017;91:1126–1145. doi: 10.1016/j.kint.2016.10.036.

24. Szeto HH, Liu S, Soong Y, Birk AV. Improving mitochondrial bioenergetics under ischemic conditions increases warm ischemia tolerance in the kidney. *Am J Physiol Renal Physiol*. 2015;308:F11–F21. doi: 10.1152/ajprenal.00366.2014.
25. Glocviczki ML, Glockner J, Gomez SI, Romero JC, Lerman LO, McKusick M, Textor SC. Comparison of 1.5 and 3 T BOLD MR to study oxygenation of kidney cortex and medulla in human renovascular disease. *Invest Radiol*. 2009;44:566–571. doi: 10.1097/RLI.0b013e3181b4c1e8.
26. Textor SC, Turner ST. Renal vascular response to sodium loading in sons of hypertensive parents. *Hypertension*. 1991;17(6 pt 2):982–988.
27. Wilson DM, Bergert JH, Larson TS, Liedtke RR. GFR determined by non-radiolabeled iothalamate using capillary electrophoresis. *Am J Kidney Dis*. 1997;30:646–652.
28. Textor SC, Glockner JF, Lerman LO, Misra S, McKusick MA, Riederer SJ, Grande JP, Gomez SI, Romero JC. The use of magnetic resonance to evaluate tissue oxygenation in renal artery stenosis. *J Am Soc Nephrol*. 2008;19:780–788. doi: 10.1681/ASN.2007040420.
29. Lerman LO, Taler SJ, Textor SC, Sheedy PF II, Stanson AW, Romero JC. Computed tomography-derived intrarenal blood flow in renovascular and essential hypertension. *Kidney Int*. 1996;49:846–854.
30. Daghini E, Primak AN, Chade AR, Krier JD, Zhu XY, Ritman EL, McCollough CH, Lerman LO. Assessment of renal hemodynamics and function in pigs with 64-section multidetector CT: comparison with electron-beam CT. *Radiology*. 2007;243:405–412. doi: 10.1148/radiol.2432060655.
31. Zhu XY, Chade AR, Rodriguez-Porcel M, Bentley MD, Ritman EL, Lerman A, Lerman LO. Cortical microvascular remodeling in the stenotic kidney: role of increased oxidative stress. *Arterioscler Thromb Vasc Biol*. 2004;24:1854–1859. doi: 10.1161/01.ATV.0000142443.52606.81.
32. Chade AR, Rodriguez-Porcel M, Grande JP, Zhu X, Sica V, Napoli C, Sawamura T, Textor SC, Lerman A, Lerman LO. Mechanisms of renal structural alterations in combined hypercholesterolemia and renal artery stenosis. *Arterioscler Thromb Vasc Biol*. 2003;23:1295–1301. doi: 10.1161/01.ATV.0000077477.40824.52.
33. Urbieto-Caceres VH, Lavi R, Zhu XY, Crane JA, Textor SC, Lerman A, Lerman LO. Early atherosclerosis aggravates the effect of renal artery stenosis on the swine kidney. *Am J Physiol Renal Physiol*. 2010;299:F135–F140. doi: 10.1152/ajprenal.00159.2010.
34. Eirin A, Zhu XY, Urbieto-Caceres VH, Grande JP, Lerman A, Textor SC, Lerman LO. Persistent kidney dysfunction in swine renal artery stenosis correlates with outer cortical microvascular remodeling. *Am J Physiol Renal Physiol*. 2011;300:F1394–F1401. doi: 10.1152/ajprenal.00697.2010.
35. Yellon DM, Hausenloy DJ. Myocardial reperfusion injury. *N Engl J Med*. 2007;357:1121–1135. doi: 10.1056/NEJMr071667.
36. Murphy E, Steenbergen C. Mechanisms underlying acute protection from cardiac ischemia-reperfusion injury. *Physiol Rev*. 2008;88:581–609. doi: 10.1152/physrev.00024.2007.
37. Schug ZT, Gottlieb E. Cardiolipin acts as a mitochondrial signalling platform to launch apoptosis. *Biochim Biophys Acta*. 2009;1788:2022–2031. doi: 10.1016/j.bbame.2009.05.004.
38. Dai DF, Chen T, Szeto H, Nieves-Cintrón M, Kutayavin V, Santana LF, Rabinovitch PS. Mitochondrial targeted antioxidant peptide ameliorates hypertensive cardiomyopathy. *J Am Coll Cardiol*. 2011;58:73–82. doi: 10.1016/j.jacc.2010.12.044.
39. Saad A, Wang W, Herrmann SM, Glockner JF, Mckusick MA, Misra S, Bjarnason H, Lerman LO, Textor SC. Atherosclerotic renal artery stenosis is associated with elevated cell cycle arrest markers related to reduced renal blood flow and postcontrast hypoxia. *Nephrol Dial Transplant*. 2016;31:1855–1863. doi: 10.1093/ndt/gfw265.
40. Kashani K, Al-Khafaji A, Ardiles T, Artigas A, Bagshaw SM, Bell M, Bihorac A, Birkhahn R, Cely CM, Chawla LS, Davison DL, Feldkamp T, Forni LG, Gong MN, Gunnerson KJ, Haase M, Hackett J, Honore PM, Hoste EA, Joannes-Boyau O, Joannidis M, Kim P, Koyner JL, Laskowitz DT, Lissauer ME, Marx G, McCullough PA, Mullaney S, Ostermann M, Rimmelé T, Shapiro NI, Shaw AD, Shi J, Sprague AM, Vincent JL, Vinsonneau C, Wagner L, Walker MG, Wilkerson RG, Zacharowski K, Kellum JA. Discovery and validation of cell cycle arrest biomarkers in human acute kidney injury. *Crit Care*. 2013;17:R25. doi: 10.1186/cc12503.
41. Bihorac A, Chawla LS, Shaw AD, Al-Khafaji A, Davison DL, Demuth GE, Fitzgerald R, Gong MN, Graham DD, Gunnerson K, Heung M, Jortani S, Kleerup E, Koyner JL, Krell K, Letourneau J, Lissauer M, Miner J, Nguyen HB, Ortega LM, Self WH, Sellman R, Shi J, Straseski J, Szalados JE, Wilber ST, Walker MG, Wilson J, Wunderink R, Zimmerman J, Kellum JA. Validation of cell-cycle arrest biomarkers for acute kidney injury using clinical adjudication. *Am J Respir Crit Care Med*. 2014;189:932–939. doi: 10.1164/rccm.201401-0077OC.
42. Meersch M, Schmidt C, Van Aken H, Martens S, Rossaint J, Singbartl K, Görllich D, Kellum JA, Zarbock A. Urinary TIMP-2 and IGFBP7 as early biomarkers of acute kidney injury and renal recovery following cardiac surgery. *PLoS One*. 2014;9:e93460. doi: 10.1371/journal.pone.0093460.
43. Roudkenar MH, Halabian R, Bahmani P, Roushandeh AM, Kuwahara Y, Fukumoto M. Neutrophil gelatinase-associated lipocalin: a new antioxidant that exerts its cytoprotective effect independent on Heme Oxygenase-1. *Free Radic Res*. 2011;45:810–819. doi: 10.3109/10715762.2011.581279.
44. Devarajan P. Update on mechanisms of ischemic acute kidney injury. *J Am Soc Nephrol*. 2006;17:1503–1520. doi: 10.1681/ASN.2006010017.
45. Kloner RA, Hale SL, Dai W, Gorman R, Shuto T, Koomalsingh KJ, Gorman JH III, Sloan RC, Frasier CR, Watson CA, Bostian PA, Kypson AP, Brown DA. Reduction of ischemia/reperfusion injury with Bendavia, a mitochondria-targeting cytoprotective peptide. *J Am Heart Assoc*. 2012;1:e001644. doi: 10.1161/JAHA.112.001644.
46. Dai W, Shi J, Gupta RC, Sabbah HN, Hale SL, Kloner RA. Bendavia, a mitochondria-targeting peptide, improves postinfarction cardiac function, prevents adverse left ventricular remodeling, and restores mitochondria-related gene expression in rats. *J Cardiovasc Pharmacol*. 2014;64:543–553. doi: 10.1097/FJC.0000000000000155.
47. Eirin A, Williams BJ, Ebrahimi B, Zhang X, Crane JA, Lerman A, Textor SC, Lerman LO. Mitochondrial targeted peptides attenuate residual myocardial damage after reversal of experimental renovascular hypertension. *J Hypertens*. 2014;32:154–165. doi: 10.1097/HJH.0b013e318283658a53.
48. Vivier PH, Storey P, Chandarana H, Yamamoto A, Tantillo K, Khan U, Zhang JL, Sigmund EE, Rusinek H, Babb JS, Bubenheim M, Lee VS. Renal blood oxygenation level-dependent imaging: contribution of R2 to R2\* values. *Invest Radiol*. 2013;48:501–508. doi: 10.1097/RLI.0b013e3182823591.
49. Lenhard DC, Frisk AL, Lengsfeld P, Pietsch H, Jost G. The effect of iodinated contrast agent properties on renal kinetics and oxygenation. *Invest Radiol*. 2013;48:175–182. doi: 10.1097/RLI.0b013e31827b70f9.

## Phase 2a Clinical Trial of Mitochondrial Protection (Elamipretide) During Stent Revascularization in Patients With Atherosclerotic Renal Artery Stenosis

Ahmed Saad, Sandra M.S. Herrmann, Alfonso Eirin, Christopher M. Ferguson, James F. Glockner, Haraldur Bjarnason, Michael A. McKusick, Sanjay Misra, Lilach O. Lerman and Stephen C. Textor

*Circ Cardiovasc Interv.* 2017;10:

doi: 10.1161/CIRCINTERVENTIONS.117.005487

*Circulation: Cardiovascular Interventions* is published by the American Heart Association, 7272 Greenville Avenue, Dallas, TX 75231

Copyright © 2017 American Heart Association, Inc. All rights reserved.

Print ISSN: 1941-7640. Online ISSN: 1941-7632

The online version of this article, along with updated information and services, is located on the World Wide Web at:

<http://circinterventions.ahajournals.org/content/10/9/e005487>

**Permissions:** Requests for permissions to reproduce figures, tables, or portions of articles originally published in *Circulation: Cardiovascular Interventions* can be obtained via RightsLink, a service of the Copyright Clearance Center, not the Editorial Office. Once the online version of the published article for which permission is being requested is located, click Request Permissions in the middle column of the Web page under Services. Further information about this process is available in the [Permissions and Rights Question and Answer](#) document.

**Reprints:** Information about reprints can be found online at:  
<http://www.lww.com/reprints>

**Subscriptions:** Information about subscribing to *Circulation: Cardiovascular Interventions* is online at:  
<http://circinterventions.ahajournals.org/subscriptions/>